Infrared Frequency-Modulation Probing of Product Formation in Alkyl + O_2 Reactions: III. The Reaction of Cyclopentyl Radical (*c*-C_5H_9) with O_2 between 296 and 723 K

John D. DeSain and Craig A. Taatjes*

Combustion Research Facility, Mail Stop 9055, Sandia National Laboratories, Livermore, California 94551-0969

Received: January 29, 2001; In Final Form: April 12, 2001

The production of HO_2 from the reaction of *c*-$C_5H_9 + O_2$ has been investigated as a function of temperature (296−723 K) by using laser photolysis/CW infrared frequency modulation spectroscopy. The HO_2 yield is derived by comparison with the $Cl_2/CH_3OH/O_2$ system and is corrected to account for HO_2 signal loss due to competing reactions involving HO_2 radical and the adduct *c*-$C_5H_9O_2$. The time behavior of the HO_2 signal following cyclopentyl radical formation displays two separate components. The first component is a prompt production of HO_2, which increases with temperature and is the only component observed between 296 and 500 K. The yield from the prompt production rises from less than 1% at 296 K to ∼23% at 693 K. At temperatures above 500 K a second slower rise in the HO_2 signal is also observed. The production of HO_2 on a slower time scale is attributable to cyclopentylperoxy radical decomposition. The total HO_2 yield, including the contribution from the slower rise, increases dramatically with temperature from ∼2% at 500 K to ∼100% at 683 K. From 683 to 723 K the total HO_2 yield remains constant. The second slower rise accounts for a majority of the product formation at these higher temperatures. The biexponential time behavior of the HO_2 production from *c*-$C_5H_9 + O_2$ is similar to that previously observed in studies of $C_2H_5 + O_2$ and $C_3H_7 + O_2$ reactions. The rate of formation for delayed HO_2 production from *c*-$C_5H_9 + O_2$ is larger than the rate of formation from either $C_2H_5 + O_2$ or $C_3H_7 + O_2$ at each temperature. However, apparent activation energies, obtained by an Arrhenius plot of the rates of formation for delayed HO_2 formation, are very similar for the three systems ($C_2H_5 + O_2$, $C_3H_7 + O_2$, and *c*-$C_5H_9 + O_2$). The results suggest a similar coupled mechanism for HO_2 production in the $C_2H_5 + O_2$, $C_3H_7 + O_2$, and *c*-$C_5H_9 + O_2$ reactions, with concerted elimination of HO_2 from the RO_2 radical responsible for HO_2 + alkene production.

Introduction

Alkyl radical (R) reactions with oxygen are critical in understanding many combustion systems. Studies of $R + O_2$ have focused mainly on understanding the complex mechanisms involved in smaller straight-chained alkyl radical (ethyl and propyl) reactions with O_2. Recently more focus has been placed on studying the oxidation of larger cyclic alkanes. The oxidation of cyclopentane has been studied by two separate groups.[1,2] If the reaction of the cyclopentyl radical (*c*-C_5H_9) with O_2 is similar to other $R + O_2$ reactions, then the major product channels should be

$$c\text{-}C_5H_9 + O_2 \overset{M}{\longleftrightarrow} c\text{-}C_5H_9O_2 \quad (1a)$$

$$\rightarrow c\text{-}C_5H_8 + HO_2 \quad (1b)$$

$$\rightarrow c\text{-}C_5H_8O(1,2\text{-epoxycyclopentane}) + OH \quad (1c)$$

where reactions 1b and 1c include possible formation from a *c*-$C_5H_9O_2$ intermediate. Reaction 1b appears to be favored at temperatures between 673 and 873 K as the two previous studies[1,2] agree that the major product of this reaction is cyclopentene (*c*-C_5H_8).

Simon et al.[1] studied the oxidation of cyclopentane at 873 K and observed product formation in a jet-stirred flow reaction vessel by using gas chromatography. They observed products from reaction pathway 1b (*c*-C_5H_8), but do not report any products from pathway 1c. They postulate that the other products (H_2, CH_4, C_2H_4, C_3H_6, 1,3-C_4H_6) observed are principally produced by decomposition of the cyclopentyl radical (*c*-C_5H_9):

$$c\text{-}C_5H_9 \longrightarrow \begin{array}{c} C_2H_4 + C_3H_6 \\ \uparrow \\ 1\text{-}C_5H_9 \\ \downarrow O_2 \\ C_2H_4, C_4H_6, \text{aldehydes} \end{array} \longrightarrow CH_4 + C_4H_6 \quad (2)$$

They propose that cyclopentene is produced via the following mechanism:

$$c\text{-}C_5H_9 + O_2 \overset{[M]}{\longleftrightarrow} c\text{-}C_5H_9O_2 \rightarrow c\text{-}C_5H_8OOH \rightarrow c\text{-}C_5H_8 + HO_2 \quad (3)$$

Simon et al.[1] used Schemes 2 and 3 together to fit the formation of four experimentally observed products (H_2O, C_2H_4, *c*-C_5H_6, and *c*-C_5H_8).

Handford-Styring and Walker[2] also used gas-phase chromatography/mass spectrometry to observe product formation from cyclopentane oxidation. Once again *c*-C_5H_8 was observed as a primary product, along with smaller amounts of acrolein (CH_2-$CHCHO$), 1,2-epoxycyclopentane (*c*-C_5H_8O), ethylene (C_2H_4), cyclopenta-1,3-diene (*c*-C_5H_6), carbon monoxide (CO), and trace amounts of propene (C_3H_6) and buta-1,3-diene (C_4H_6). Cyclo-

* Author to whom correspondence should be addressed

10.1021/jp010364t CCC: $20.00
Published on Web 06/19/2001

pentene is found to be the dominant initial product at O_2 pressures greater than 1 Torr. Handford-Styring and Walker used a formally direct step (i.e., without intervening isomerization to C_5H_8OOH) for the formation of the cyclopentene to model their results:

$$c\text{-}C_5H_9 + O_2 \rightarrow c\text{-}C_5H_8 + HO_2 \qquad (4)$$

At low oxygen pressures (<1 Torr O_2) C_2H_4 formation became significant, indicating that C_2H_4 is formed from the competing reaction of c-C_5H_9 decomposition. Also, Handford-Styring and Walker[2] observed an additional source of C_2H_4 formation, which they attributed to adduct decomposition, similar to the HO_2 formation scheme above. This additional reaction channel

$$\begin{array}{c} c\text{-}C_5H_8O + OH \\ \uparrow \\ c\text{-}C_5H_9 + O_2 \xleftrightarrow{[M]} c\text{-}C_5H_9O_2 \rightarrow c\text{-}C_5H_8OOH \rightarrow C_2H_4 + CH_2CHCHO + OH \\ \downarrow \\ \textit{removal} \end{array} \qquad (5)$$

explains the appearance of acrolein and 1,2-epoxycyclopentane as well as other minor products.

We have recently investigated the reactions of ethyl (C_2H_5)[3] and propyl (C_3H_7),[4] with O_2. The propyl + O_2[4−10] and ethyl + O_2[3,11−23] reactions have been much more extensively studied than reactions involving larger alkyl radicals. The HO_2 formation from C_2H_5 + O_2 and C_3H_7 + O_2 reactions are very similar. The HO_2 + alkene channel is the dominant bimolecular product channel observed at temperatures between 296 and 683 K for both C_2H_5 + O_2 and C_3H_7 + O_2. For both reactions, the HO_2 yield exhibits a biexponential time behavior with both a very fast direct component and a much slower delayed component. The prompt component of the yield increases with temperature, while the delayed component of the yield increases sharply from 550 to 683 K. The prompt HO_2 yield is slightly larger for C_2H_5 + O_2 than C_3H_7 + O_2 in the temperature region studied. Both reactions show a similar increase in total yield with temperature, changing from ∼5% at 500 K to nearly 100% at 683 K. The delayed component makes a large contribution to the total yield at these higher temperature, while having no significant contribution at temperatures below 550 K. The rate of formation for delayed HO_2 production from C_3H_7 + O_2 is slightly larger than for C_2H_5 + O_2 at each temperature. Apparent activation energies, obtained by an Arrhenius plot of the rates of formation of the delayed HO_2 yield, are very similar for the two systems, ∼25 kcal mol^{-1} and ∼26 kcal mol^{-1} for C_2H_5 + O_2 and C_3H_7 + O_2, respectively. The HO_2 yield and time behavior for C_2H_5 + O_2 derived from recent master equation calculations by Miller, Klippenstein, and Robertson,[20] based on quantum calculations of the transition state for the concerted HO_2 elimination from the ethylperoxy radical,[23] also showed excellent agreement with the experimental results.[3]

This study investigates the yield and time behavior of the HO_2 formation from the c-C_5H_9 + O_2 reaction at elevated temperatures. Both Handford-Styring and Walker[2] and Simon et al.[1] used gas chromatography to measure stable products of the cyclopentane oxidation. Using this method they were able to measure stable product yields, but not the time dependence of the product formation. In these studies the time behavior of HO_2 formation from the reaction of c-C_5H_9 + O_2 is directly observed by using infrared frequency modulation spectroscopy. The time profile of the HO_2 formation permits separation of initially formed "prompt" HO_2 from the product of redissociation of the cyclopentylperoxy adduct. In this way the increase in HO_2 + c-C_5H_8 yield above 500 K is unambiguously assigned to c-$C_5H_9O_2$ dissociation. The rate of formation for the delayed formation of HO_2 is similar to that observed in C_2H_5 + O_2 and C_3H_7 + O_2, which suggests that the three reactions have a similar reaction mechanism for HO_2 + alkene formation.

Experiment

The reaction of c-C_5H_9 + O_2 is investigated by using a modification of the laser photolysis/CW infrared long path absorption (LP/CWIRLPA) method employed in previous experiments.[3,4,24−28] The Cl is generated by photolysis of Cl_2 at 355 nm, and the c-C_5H_9 is generated by subsequent Cl abstraction from cyclopentane. The c-C_5H_9 radical then reacts with O_2 to produce the HO_2 radical.

$$Cl_2 \xrightarrow{h\nu\ (355\ nm)} 2Cl\bullet \qquad (6a)$$

$$Cl\bullet + c\text{-}C_5H_{10} \rightarrow c\text{-}C_5H_9\bullet + HCl \qquad (6b)$$

$$c\text{-}C_5H_9\bullet + O_2 \rightarrow \text{products} \qquad (1)$$

The O_2 concentration is kept at least 30 times greater than the Cl_2 concentration in order to minimize the effects of the competing chain reaction of Cl_2 with c-C_5H_9.

The progress of reaction 1b is monitored by two-tone frequency modulation (FM) spectroscopy on the overtone of the O−H stretch in HO_2 near 1.5 μm by using a tunable diode laser. The detection sensitivity decreases at higher temperatures because of increases in the vibrational and rotational partition functions, and the concomitant quantum state dilution. The diode laser output is passed multiple times (17 passes) through a Herriott-type flow cell.[29,30] The flow cell is 1.3 m long with CaF_2 windows and is surrounded by a commercial ceramic-fiber heater capable of reaching temperatures in excess of 1200 K.

The gold-coated spherical mirrors that comprise the Herriott cell are located outside the flow cell and are separated by a distance of approximately 1.5 m. The photolysis beam, a 5 ns pulse from a Nd:YAG laser at 355 nm, passes through the center of the front Herriott mirror. It travels on axis through the quartz flow cell and then passes through the center of the back Herriott mirror. The IR probe beam enters off axis through a notch in the back Herriott mirror and is multipassed through the flow cell. The beam traverses a circular pattern around the outer edge of the Herriott mirrors, while mapping out a smaller circle in the center of the cell. Finally, the probe exits from a notch in the front Herriott mirror. After exiting, the probe beam is focused onto a detector. This arrangement allows the IR probe to overlap the UV photolysis beam only in the center of the flow cell, where the temperature is more readily controlled. By using this multipass arrangement the effective path length (i.e., overlapping path of the photolysis and probe) is about 9 m.

The relative yield of the HO_2 radical produced by the reaction is monitored by comparison with the corresponding HO_2 yield from the reaction of CH_2OH + O_2. This reaction produces a 100% yield of HO_2 as a product over the temperature range of concern.[31] The CH_2OH is produced by Cl abstraction of hydrogen from methanol.

$$Cl_2 \xrightarrow{h\nu\ (355\ nm)} 2Cl\bullet \qquad (7a)$$

$$CH_3OH + Cl\bullet \rightarrow CH_2OH\bullet + HCl \quad 100\% \qquad (7b)$$

$$CH_2OH\bullet + O_2 \rightarrow CH_2O + HO_2\bullet \quad 100\% \qquad (7c)$$

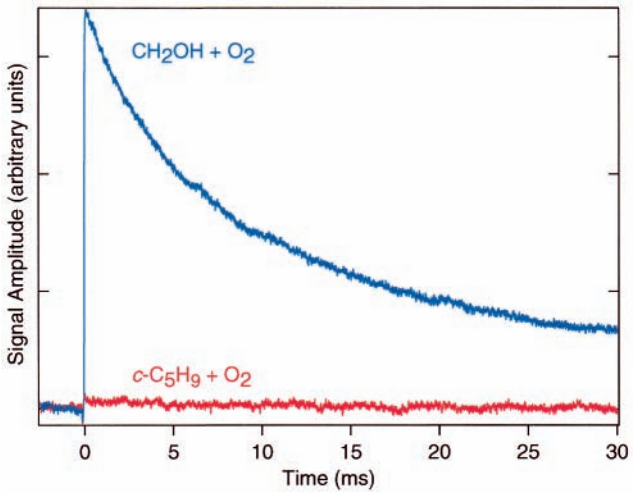

Figure 1. Time-resolved infrared FM signals for HO_2 taken at 453 K and 40.0 Torr. The larger amplitude (blue) trace is the HO_2 signal from the reference reaction of $CH_2OH + O_2$; the smaller amplitude (red) trace is the HO_2 signal from c-$C_5H_9 + O_2$.

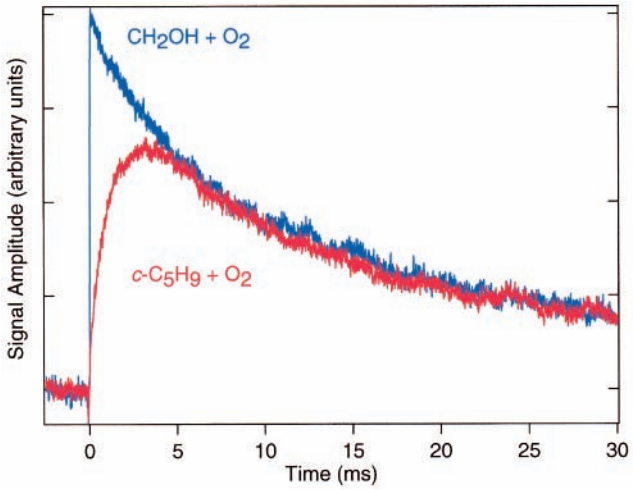

Figure 2. Time-resolved infrared FM signals for HO_2 taken at 638 K and 56.2 Torr. The larger amplitude (blue) trace is the HO_2 signal from the reference reaction of $CH_2OH + O_2$; the smaller amplitude (red) trace is the HO_2 signal from c-$C_5H_9 + O_2$.

The experiments are conducted by first observing the HO_2 signal produced from the $CH_2OH + O_2$ reaction. Then the methanol is replaced with a nearly equal concentration of cyclopentane and the HO_2 signal from the c-$C_5H_9 + O_2$ reaction is observed. The yield is then obtained by comparison of the intensities of the two resulting HO_2 signals. To relate the observed quantities to characteristics of the reaction, corrections must be made for the removal reactions of HO_2, as well as for certain side reactions, as discussed below. Typical gas concentrations are $[O_2] = 6.6 \times 10^{16}$ cm^{-3}, $[Cl_2] = 2.1 \times 10^{15}$ cm^{-3}, and 8.0×10^{15} cm^{-3} of either cyclopentane or methanol. Helium is added to a total gas density of 8.5×10^{17} cm^{-3}.

Analysis

The HO_2 signal from c-$C_5H_9 + O_2$ is similar to the signal observed from the $C_2H_5 + O_2$ and $C_3H_7 + O_2$ studies. At low temperatures, <500 K, very little HO_2 is observed. The HO_2 observed below 500 K appears rapidly after the photolysis pulse (see Figure 1), with a rise time faster than the experimental resolution of ~10 μs, (limited by the low-pass filter used in the two-tone FM method). Above 500 K a second slower HO_2 signal is observed. Figure 2 shows the HO_2 signal from c-$C_5H_9 + O_2$ and $CH_2OH + O_2$ at 638 K. In Figure 2 the HO_2 signal shows two components: an initial sharp rise that is not resolved and a second much slower rise. Determining the fraction of HO_2 that appears via this delayed mechanism requires correction for the ongoing removal of HO_2 by self-reaction and by reactions with other radical species.

As in previous studies,[3,4] an iterative integration technique is employed to correct the signal for the loss of HO_2. Correction for the self-reaction uses only information inherent to the HO_2 signals from $CH_2OH + O_2$ and c-$C_5H_9 + O_2$, and requires no assumed rate coefficients. The HO_2 signal generated from the $CH_2OH + O_2$ reaction decays by a second-order kinetic process dominated by the $HO_2 + HO_2$ recombination reaction,

$$HO_2 + HO_2 \rightarrow \text{products} \qquad (8)$$

The time profile of the HO_2 signal from the reference reaction is given by

$$I_{\text{ref}}(t) = \alpha[HO_2]_t = \frac{\alpha[HO_2]_0}{1 + 2k_8 t[HO_2]_0} \qquad (9)$$

where α is a constant relating the observed FM signal to HO_2 concentration. A plot of the inverse of the reference HO_2 signal vs time gives a line with slope $2k_8/\alpha$. Since the temperature-dependent line-strength of the probe transition is unknown, the absolute value of k_8 remains undetermined in these experiments; however, the analysis requires only the phenomenological rate coefficient $2k_8/\alpha$. The differential equation governing the HO_2 concentration in the cyclopentyl $+ O_2$ reaction can be written as

$$\frac{d}{dt}[HO_2] = R_{\text{production}} - 2k_8[HO_2]^2 - R_{\text{removal}} \qquad (10)$$

where $R_{\text{production}}$ is the effective time-dependent rate of HO_2 production and R_{removal} is the effective time-dependent rate for removal of HO_2 by processes besides self-reaction. Determining the time-resolved production of HO_2 from reaction 1, denoted $R_{\text{production}}$, is the aim of the measurement. Equation 10 has the formal solution

$$[HO_2]_t = \int_0^t R_{\text{production}}(x)\,dx - 2k_8\int_0^t [HO_2]_x^2\,dx - \int_0^t R_{\text{removal}}(x)\,dx \qquad (11)$$

The time-dependent FM signal, $I(t)$, from HO_2 produced in reaction 1 is related by the detection constant α to the HO_2 concentration:

$$I(t) = \alpha\int_0^t R_{\text{production}}(x)\,dx - 2\alpha k_8\int_0^t [HO_2]_x^2\,dx - \alpha\int_0^t R_{\text{removal}}(x)\,dx \qquad (12)$$

The integrated profiles method[32−34] uses this formal solution along with the measured time-resolved relative concentrations to correct for known rate processes. The quantity $2k_8/\alpha$ is known from the reference reaction, and the time profile of the HO_2 FM signal from reaction 1 has been measured: $I(t) = \alpha[HO_2]_t$. The self-reaction term in the expression for the FM signal amplitude, the second term on the right in eq 12, can be replaced by a time integral of the observed signal:

$$\alpha\int_0^t R_{\text{production}}(x)\,dx = I(t) + \frac{2k_8}{\alpha}\int_0^t I(x)^2\,dx + \alpha\int_0^t R_{\text{removal}}(x)\,dx \quad (14)$$

If HO_2 recombination were the only loss mechanism of significance, then R_{removal} would be equal to zero and all parameters in eq 14 are measured directly by the experiment. This assumption produces a lower bound to the actual HO_2 production rate, since additional corrections for HO_2 signal lost by other mechanisms (R_{removal}) will increase the amplitude of the final "corrected" time profile. The yields obtained by this assumption thus produce a lower limit to the true yields, but have the advantage of being dependent only on data acquired in this experiment.

Whereas the data necessary for removing the contributions of HO_2 self-reaction are inherent in the measurements themselves, relating the phenomenological yields to the time-dependent HO_2 production rate requires additional modeling to account for the R_{removal} processes. Under the conditions of the present experiments, R_{removal} reflects principally the reaction of HO_2 with c-$C_5H_9O_2$ radicals,

$$HO_2 + c\text{-}C_5H_9O_2 \rightarrow \text{products} \quad (15)$$

so that $R_{\text{removal}} \approx k_{15}[c\text{-}C_5H_9O_2]_t[HO_2]_t$. The c-$C_5H_9O_2 + HO_2$ reaction has been studied previously, and k_{15} can be estimated from literature expressions.[35,36] Since the actual correction method uses the observed signals, not absolute concentrations, the value for the relevant rate coefficients must be scaled by the (unknown) factor α. The values for the rate coefficients (listed in Table 1) are therefore scaled to the literature value of the HO_2 recombination rate coefficient (whose phenomenological rate coefficient, $2k_8/\alpha$, is measured in the $CH_2OH + O_2$ reference reaction), e.g.,

$$\left(\frac{k_{15}}{\alpha}\right) = \left(\frac{2k_8}{\alpha}\right)\left(\frac{k_{15}}{k_8}\right)\frac{1}{2} \quad (16)$$

Information on the concentration of c-$C_5H_9O_2$ is needed as well. Unfortunately there is no direct measure of the time behavior of the cyclopentylperoxy radical concentration. An estimate can be obtained assuming that all cyclopentyl radicals react to produce either HO_2 or c-$C_5H_9O_2$. This assumption is good if reaction 1c is small,[2] and if the steady-state for reaction 1a favors the products, which should be the case under the high-$[O_2]$ conditions of the present experiments, if the c-$C_5H_9 + O_2 \leftrightarrow c$-$C_5H_9O_2$ equilibrium is similar to that of other alkyl radicals C_2H_5, i-C_3H_7, or t-$C_4H_9 + O_2$ ($\Delta H \sim 36$ kcal mol^{-1} and $\Delta S \sim 37$ cal mol^{-1} K^{-1}).[16] Then immediately after the fast establishment of the steady-state concentration $[c\text{-}C_5H_9O_2] \approx [c\text{-}C_5H_9]_0 - [HO_2]$. Note that above 668 K the raw yield obtained by correcting for only $HO_2 + HO_2$ already produces a nearly 100% yield and this correction becomes insignificant.

The self-reaction of the cyclopentylperoxy is another removal mechanism for c-$C_5H_9O_2$:

$$c\text{-}C_5H_9O_2 + c\text{-}C_5H_9O_2 \rightarrow \text{products} \quad (17)$$

The c-$C_5H_9O_2$ recombination rate constant (k_{17}) has been found to be dependent on O_2 concentration. Rowley et al.[37] report a low O_2 concentration limit (<1 Torr O_2) of $1.3 \pm 0.4 \times 10^{-14}$ $e^{(188 \pm 83\ K/T)}$, whereas the high O_2 limit (>50 Torr O_2) was found to be $2.9 \pm 0.8 \times 10^{-13}$ $e^{[-(555 \pm 77\ K)/T]}$. The present experimental conditions are nearer the lower limit, and that value has been chosen for k_{17}.

TABLE 1: Rate Coefficients Used to Obtain the Relative Rates Used to Correct for HO_2 Loss from the c-$C_5H_9O_2$ + HO_2 Reaction[a]

reaction	rate constant (cm^3 molecule^{-1} s^{-1})
$HO_2 + HO_2$[14]	$k_8 = 4.5 \times 10^{-32}$ [M] + $2.2\ 10^{-13}$ $e^{(599\ K/T)}$
c-$C_5H_9O_2 + HO_2$[36]	$k_{15} = 3.2[+1.5-1.1] \times 10^{-13}$ $e^{(1150 \pm 200\ K/T)}$
c-$C_5H_9O_2 + c$-$C_5H_9O_2$[37]	$k_{17} = 1.3 \pm 0.4 \times 10^{-14}$ $e^{(188 \pm 83\ K/T)}$

[a] The evaluated rate coefficient for the HO_2 self-reaction is used to scale the value for c-$C_5H_9O_2 + HO_2$ and c-$C_5H_9O_2 + c$-$C_5H_9O_2$.

By using reactions 1,8,15, and 17, a formal solution to the kinetic equations can be constructed that allows recursive extraction of a corrected HO_2 profile. The equation for the observed HO_2 FM signal is modified to reflect that R_{removal} is dominated by reaction with cyclopentylperoxy radicals, and the kinetic equations are recast as equations by using the observed signals (i.e., effectively using signal amplitude as a concentration unit):

$$A \equiv \alpha[c\text{-}C_5H_9O_2]_t = I_{\text{ref}}(0) - \alpha\int_0^t R_{\text{production}}(x)\,dx - \frac{2k_{17}}{\alpha}\int_0^t(\alpha[c\text{-}C_5H_9O_2]_x)^2\,dx - \frac{k_{15}}{\alpha}\int_0^t \alpha[c\text{-}C_5H_9O_2]I(x)\,dx \quad (18)$$

$$B \equiv \alpha\int_0^t R_{\text{production}}(x)\,dx = I(t) + \frac{2k_8}{\alpha}\int_0^t I(x)^2\,dx + \frac{k_{15}}{\alpha}\int_0^t \alpha[c\text{-}C_5H_9O_2]_x I(x)\,dx \quad (19)$$

We initially assume $A_{(0)} = 0$, and then calculate successive approximations to the quantities A and B by using the following equations:

$$B_{(n)}(t) = I(t) + \frac{2k_8}{\alpha}\int_0^t I(x)^2\,dx + \frac{k_{15}}{\alpha}\int_0^t A_{(n-1)}I(x)\,dx \quad (20)$$

$$A_{(n)}(t) = (I_{\text{ref}}(0) - B_{(n)}) - \frac{2k_{17}}{\alpha}\int_0^t (I_{\text{ref}}(0) - B_{(n)})^2\,dx - \frac{k_{15}}{\alpha}\int_0^t (I_{\text{ref}}(0) - B_{(n)})I(x)\,dx \quad (21)$$

Iteration of these equations converges to a solution for B that represents the production of HO_2 from reaction 1 that gives rise to the observed signal under the conditions of the model. The yields extracted from this procedure are necessarily larger than or equal to the raw yields taken directly from the data (corrected only for HO_2 self-reaction).

Results

HO_2 Yields. Figure 3 shows the HO_2 signals from both the $CH_2OH + O_2$ and c-$C_5H_9 + O_2$ reactions at 638 K with the loss of signal due to reactions 8 and 15 removed. The HO_2 signal from the $CH_2OH + O_2$ reaction now displays a nearly instantaneous increase in HO_2 after the UV pulse with no observable decrease in the signal over the 30 ms time window. The HO_2 production from the c-$C_5H_9 + O_2$ reaction also appears different from the signal shown in Figure 2. At the end of the second rise the amplitude approaches a plateau. The total yield can now be obtained by a comparison of final amplitude of the two signals. In practice the final HO_2 signal amplitude from the c-$C_5H_9 + O_2$ is obtained by a fit of the delayed HO_2 rise to an exponential.

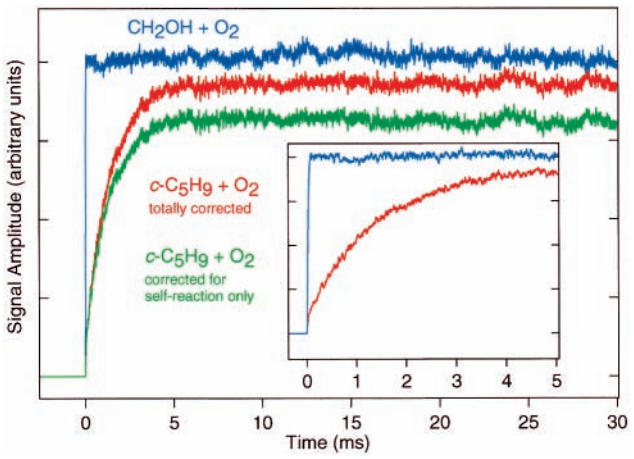

Figure 3. Correction of HO_2 FM signal by using the integrated profiles method at 638 K and 56.2 Torr. The largest amplitude trace (blue) is the HO_2 signal from the reference reaction of $CH_2OH + O_2$ after correction for HO_2 self-reaction, the dominant removal process for HO_2 in this system. The middle (red) trace is the HO_2 signal from the *c*-$C_5H_9 + O_2$ after correction accounting for both the HO_2 self-reaction and the reaction with *c*-$C_5H_9O_2$ radicals as described in the text. This trace represents the time-resolved production of HO_2 corresponding to the observed time-resolved FM signal. The lowest (green) trace is the HO_2 signal from the *c*-$C_5H_9 + O_2$ after correction accounting for only the HO_2 self-reaction. The biexponential time behavior of the HO_2 formation from *c*-$C_5H_9 + O_2$ is more clearly shown by the inner graph, which is an expansion of the first 5 ms of the middle (red) trace.

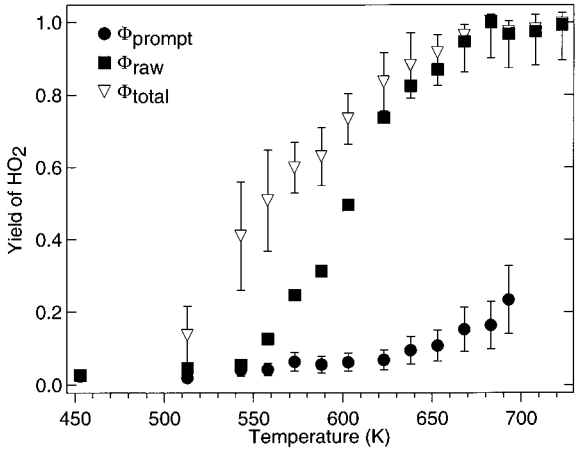

Figure 4. The measured total yield of HO_2 from the reaction of *c*-$C_5H_9 + O_2$ as a function of temperature at a constant total density of 8.5×10^{17} molecule cm^{-3}. The filled squares ■ represent the total yield assuming only HO_2 self-reaction, which is a lower bound to the true HO_2 yield. The triangles ▽ represent the yield accounting for both the HO_2 self-reaction and the reaction with *c*-$C_5H_9O_2$ radicals as described in the text. The filled circles ● represent the prompt HO_2 yield observed. Uncertainty estimates represent a combination of statistical and possible systematic errors.

The HO_2 yield at a constant total density (8.5×10^{17} cm^{-3}) and a constant partial density of O_2, Cl_2, and methanol/cyclopentane for several different temperatures is shown in Figure 4. Each point in Figure 4 represents an average of two separate measurements, except at temperatures above 668 K, which are an average of 4 measurements. The total HO_2 yield obtained by the two different correction methods is shown. The first method considers the total yield obtained by correcting only HO_2 loss due to the HO_2 self-reaction, i.e., by using only data inherent in the raw measurements themselves. This yield is a lower limit to the HO_2 yield. The second yield is obtained by correcting the HO_2 signal by considering all the reactions discussed above. The yield estimates based on both methods

TABLE 2: Yields and Rates of Production for HO_2 Production from *c*-$C_5H_9 + O_2$ at a Constant Density of 8.5×10^{17} cm^{-3}[a]

Temperature (K)	τ^{-1} (s^{-1})	Φ_{prompt}	Φ_{total}	Φ_{raw}
296		<0.01	<0.01	<0.01
338		<0.01	<0.01	<0.01
393		<0.01	<0.01	<0.01
453		0.02	0.02	0.02
513		0.02	0.14 ± 0.08	0.05
543	40 ± 35	0.04	0.41 ± 0.15	0.06
558	60 ± 35	0.04	0.51 ± 0.14	0.13
573	100 ± 35	0.06	0.60 ± 0.07	0.25
588	150 ± 50	0.06	0.63 ± 0.08	0.31
603	240 ± 50	0.06	0.73 ± 0.06	0.50
623	540 ± 60	0.07	0.84 ± 0.04	0.74
638	700 ± 60	0.09	0.88 ± 0.03	0.83
653	1080 ± 60	0.11	0.92 ± 0.05	0.87
668	1720 ± 80	0.15	0.96 ± 0.03	0.95
683	2840 ± 80	0.16	1.00 ± 0.02	1.00
693	3540 ± 140	0.23	0.97 ± 0.03	0.97
708	5570 ± 140	[b]	0.98 ± 0.04	0.97
723	6600 ± 140		1.00 ± 0.03	0.99

[a] Numbers are an average of 2 measurements for temperatures below 668 K and an average of 4 for temperatures above 668 K. The stated error bars for τ^{-1} and Φ_{total} represent propagated uncertainties introduced in the modeling, as described in the text. The estimated accuracy of the prompt yield is ±40% and is dominated by possible systematic error in the extrapolation to $t = 0$. The HO_2 yields are further subject to systematic uncertainties of ~ ±10%. See text for details. [b] Above 693 K the rapid rate of formation of the delayed HO_2 makes it too difficult to separate the delayed and prompt yield.

(corrected only for HO_2 self-reaction, and by using $R_{removal} = k_{15}[c\text{-}C_5H_9O_2]_t[HO_2]_t$) are given in Table 2 as Φ_{raw} and Φ_{total}, respectively. The total yield of HO_2 is relatively small at temperatures below 500 K. Above 500 K, a sharp increase in the total yield is observed in conjunction with a change in the time profile of the HO_2 signal. At these higher temperatures the HO_2 signal has two rises—an instantaneous rise after the laser pulse followed by a slower secondary rise. The total yield reaches ~100% by about 683 K.

The HO_2 yield below 450 K is below the ~1% detection limit of these experiments. Above 450 K an HO_2 signal is observed. At 453 K the HO_2 signal appears to be produced nearly instantaneously as shown in Figure 1. Plotted in Figure 5 is the prompt yield of HO_2 measured from the amplitude of the initial rapid rise of the HO_2 signal. The prompt yield increases slightly with increasing temperature. At higher temperatures, it is sometimes hard to discern by eye the prompt yield from the initial slow HO_2. At these temperatures the intercept of an exponential fit to the slow HO_2 production is used to obtain the prompt yield. At temperatures above 693 K the prompt and delayed production become indistinguishable. The prompt yield (Φ_{prompt}) at several temperatures is also listed in Table 2.

The time-resolved FM signal shown in Figure 3, after the correction for HO_2 self-reaction and *c*-$C_5H_9O_2 + HO_2$ reactions, is related to the production of HO_2 in reaction 1:

$$I_{eff}(t) \approx \alpha \int_0^t R_{production}(x)\, dx \qquad (22)$$

The present experiments require relatively large concentrations of O_2, since the signal size is determined by the initial Cl concentration (and hence the Cl_2 concentration), and $[O_2]$ is maintained at $30 \times [Cl_2]$. As a result, the initial rise of HO_2 from the reaction of cyclopentyl radical with O_2 is rapid and unresolved. However, the rate constant of formation, the inverse of the time constant, τ^{-1}, in the production of HO_2 can be

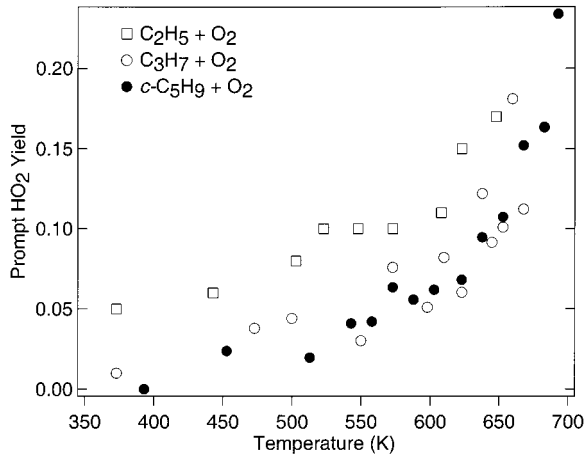

Figure 5. The temperature dependence of the "prompt" yield of HO_2 from the reactions c-$C_5H_9 + O_2$, $C_3H_7 + O_2$, and $C_2H_5 + O_2$ at constant densities of 8.5×10^{17} molecule cm^{-3}, 8.45×10^{17} molecule cm^{-3}, and 7.7×10^{17} molecule cm^{-3}, respectively. The c-$C_5H_9 + O_2$ yields from this work are represented by the filled circles ●, the $C_2H_5 + O_2$ yields (from ref 3) by the squares □, and the $C_3H_7 + O_2$ yields (from ref 4) by the open circles ○.

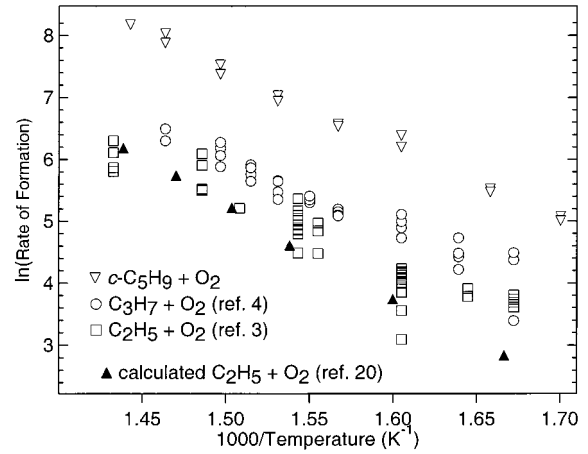

Figure 6. Arrhenius plot of the apparent rate constants of formation (τ^{-1}) for delayed production of HO_2 from the reactions c-$C_5H_9 + O_2$, $C_3H_7 + O_2$, and $C_2H_5 + O_2$ at constant densities of 8.5×10^{17} molecule cm^{-3}, 8.45×10^{17} molecule cm^{-3}, and 7.7×10^{17} molecule cm^{-3}, respectively. The c-$C_5H_9 + O_2$ rate constants represented by the open triangles ▽ are from this work. The squares □ represent the $C_2H_5 + O_2$ rates of formation from ref 3 and the open circles ○ represent the $C_3H_7 + O_2$ rates of formation from ref 4. The experimental determinations are subject to larger uncertainty at lower rate coefficient values. The filled triangles ▲ represent the rate constants of formation predicted by the master equation calculations for $C_2H_5 + O_2$ (ref 20).

measured by using an exponential fit. The rate constants are listed in Table 2. Figure 6 shows an Arrhenius plot for the rates of formation of the delayed HO_2, extracted from the effective signals after correction for self-reaction and the $HO_2 + c$-$C_5H_9O_2$ reaction (reaction 15), as a function of inverse temperature. The rate of formation displays a rapid increase from approximately 40 s^{-1} at 543 K to several thousand per second at 723 K. The lowest temperature production rates are strongly affected by the correction for reaction 15, but at higher temperatures this correction is less important and the rates of formation are independent of the details of the HO_2 removal mechanism.

The uncertainties associated with the rate coefficients used in the model to correct for the adduct + HO_2 reaction place limits on the precision of the total yields and rates obtained in this experiment. However, the raw yields are dependent only on the data measured in this experiment and thus not subject to these modeling uncertainties. At higher temperatures (≥668 K), where replacing only the loss of signal due to HO_2 recombination already produces a nearly 100% yield, modeling of the more poorly known secondary reactions has very little effect on the corrected HO_2 signal. At lower temperatures, where the slow secondary rise of the HO_2 signal is not observed, these reactions also have very little effect on the yield. From Figure 4 one can see that the raw and total yields are very similar at the extremes of the temperature range.

Uncertainties in the total yields and rates arising from uncertainty in k_8, k_{15}, and k_{17} are obtained by modeling with k_8, k_{15}, and k_{17} values that were either double or half those listed in Table 1. Since the modeling depends on rate constants relative to k_8, the maximum deviation is usually obtained when k_8 and k_{15} are changed in the opposite direction (i.e., if k_{15} is doubled then k_8 is halved). The rates show little dependence on k_{17}. The uncertainties obtained by this method are listed in Table 2 next to the total yield and rates. The lower temperature corrected yields and rates show the largest uncertainties, since they are most affected by the correction for reactions 15 and 17. The higher temperature yields show little added uncertainty from the modeling. Systematic uncertainties add an estimated ±10% relative uncertainty to the yields. The possible role of channel 1c could be systematically underestimated by these measurements, since the OH product will regenerate c-C_5H_9, as discussed below. An overall accuracy of ±40% in the prompt yield determination is estimated based on possible systematic errors in describing the HO_2 production as two separable steps as well as the statistical uncertainty in the extrapolation back to $t = 0$.

Another possible concern at the highest temperatures of this study is the effect of cyclopentyl thermal decomposition. Handford-Styring and Walker[2] have measured this decomposition rate to be $1.38 \times 10^{13} \exp(-17260\ \mathrm{K}/T)$ s^{-1}.[2] At 723 K this corresponds to a rate of ~600 s^{-1} which is still an order of magnitude smaller than the observed HO_2 formation rate constant. The major products of the decomposition reaction are the allyl radical (CH_2CHCH_2) and C_2H_4. At the temperatures of interest the allyl + O_2 reaction should form negligible HO_2 ($k = 4.15 \times 10^{-19}$ cm^3 s^{-1} at 753 K)[38] on these time scales, and any cyclopentyl radical lost to dissociation will not result in formation of HO_2. Given that the raw HO_2 yields are approximately 100% at these higher temperatures, cyclopentyl radical decomposition does not appear to be significant under the present conditions.

Discussion

The present results can be compared to previous investigations of $C_2H_5 + O_2$ and $C_3H_7 + O_2$. The total yields of HO_2 produced from $C_2H_5 + O_2$, $C_3H_7 + O_2$, and c-$C_5H_9 + O_2$ are shown in Figure 7. The HO_2 yields produced by $C_2H_5 + O_2$ and $C_3H_7 + O_2$ were previously seen to have nearly identical temperature dependence. The HO_2 yield from c-$C_5H_9 + O_2$ shows a slightly different temperature dependence. The onset of the increased production of HO_2 occurs at a lower temperature (~500 K compared to 550 K). The rise in HO_2 yield at these higher temperatures for $C_2H_5 + O_2$ has been previously modeled very successfully by a coupled reaction scheme,[3,18]

$$\begin{array}{l} C_2H_5 + O_2 \xrightarrow{k_a} C_2H_4 + HO_2 \\ C_2H_5 + O_2 \xleftrightarrow{k_b[M]} C_2H_5O_2 \xrightarrow{k_c[M]} C_2H_4 + HO_2 \\ \qquad\qquad \downarrow \\ \qquad\qquad \textit{removal} \end{array} \qquad (23)$$

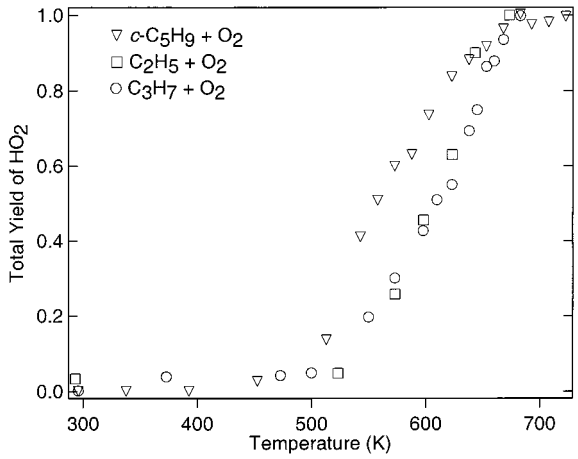

Figure 7. The open triangles ▽ represent the measured total yield of HO_2 from the reaction of c-$C_5H_9 + O_2$ as a function of temperature at a constant total density of 8.5×10^{17} molecule cm^{-3}. The squares □ represent the measured total yield of HO_2 from the reaction of $C_2H_5 + O_2$ as a function of temperature at a constant total density of 7.7×10^{17} molecule cm^{-3} (ref 3). The open circles ○ represent the measured total yield of HO_2 from the reaction of $C_3H_7 + O_2$ as a function of temperature at a constant total density of 8.45×10^{17} molecule cm^{-3} (ref 4).

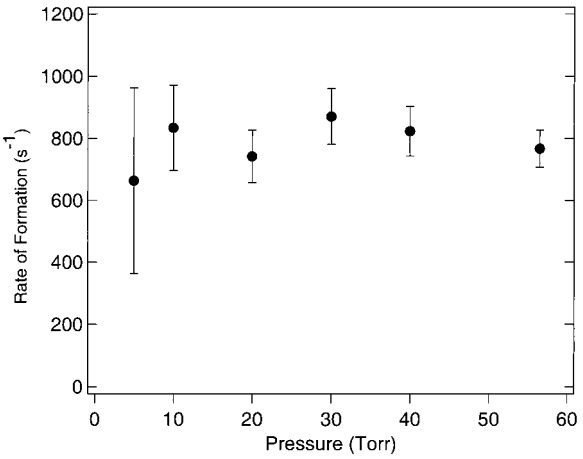

Figure 8. Pressure dependence of the rate constant of formation τ^{-1} for delayed production of HO_2 from the reaction of c-$C_5H_9 + O_2$ at 638 K and at a constant O_2 density of 6.6×10^{16} molecule cm^{-3}. Each point represents an average of 4 separate measurements.

where k_e represents concerted elimination from $C_2H_5O_2$ and k_a represents a direct production of HO_2 and ethylene from the reactants. This direct production is not strictly speaking a distinct process, but is best described as concerted elimination of the HO_2 from the excited ethylperoxy adduct prior to stabilization.[20,23] In general, the kinetics of Scheme 23 give a biexponential production of HO_2 products, where the rates of formation and amplitudes depend on all the rate coefficients of the system. This phenomenological scheme reproduces the biexponential behavior of the HO_2 yields from $C_2H_5 + O_2$. The first exponential is not resolved in these experiments and results in the appearance of prompt HO_2 formation, while the second exponential is resolved and can be fit by an exponential to obtain a rate constant of formation for the delayed HO_2, τ^{-1}. The mechanism is similar to the one used by Simon et al.[1] to describe HO_2 production from c-$C_5H_9 + O_2$, except that the reaction does not proceed through a QOOH intermediate.[2]

As shown in Figure 6 the rate constant of formation for the delayed HO_2, τ^{-1}, is larger at each temperature for c-$C_5H_9 + O_2$ than for $C_2H_5 + O_2$ or $C_3H_7 + O_2$. The larger rate of HO_2 formation for c-$C_5H_9 + O_2$ could in principle reflect different falloff behavior for the three reactions. However, the previous experiments[3,4] on $C_2H_5 + O_2$ and $C_3H_7 + O_2$ show that their rates of HO_2 formation are already pressure independent under the conditions of these experiments. The rate constant of formation with c-$C_5H_9 + O_2$ is also pressure independent at 638 K (see Figure 8), which precludes falloff effects as the source of the difference among these $R + O_2$ reactions. The difference may arise from a difference in the Arrhenius A factor for the HO_2 elimination channels. Thermochemically the A factor is related to the entropy difference between the reactant RO_2 adduct and the transition state. The adducts formed by acyclic radicals such as ethyl and propyl lose internal methyl rotation on the carbon atom in forming the five-membered (CH−OOC) ring in the transition state. In the cyclopentyl adduct these hydrogen atoms are already relatively fixed as the neighboring carbon atoms are not free to rotate. The loss of the internal rotation in the elimination from acyclic radical adducts implies a greater reduction in entropy when forming this five-membered ring than for the cyclopentyl adduct, thus giving a lower A factor.

Scheme 23 can be sufficiently described by an energetic model with one well on the potential energy surface. The $R + O_2$ reaction proceeds over a barrierless transition state to form the adduct (RO_2). There is a second transition state for the formation of HO_2 + alkene with a barrier slightly below the reactants' energy. Even in this simple formulation the observed delayed rate of formation cannot be described as an elementary rate constant in the reaction, but will depend on all of the rate coefficients. Thus the measured activation energy is a phenomenological activation energy for the whole mechanism leading to delayed product formation. The apparent activation energies of the three reactions, as seen in an Arrhenius plot (Figure 6), are very similar, 25 kcal mol^{-1}, 26 kcal mol^{-1}, and 23 kcal mol^{-1} for $C_2H_5 + O_2$, $C_3H_7 + O_2$, and c-$C_5H_9 + O_2$, respectively. (Because of the large uncertainty in the lowest temperature HO_2 formation rate coefficients, the estimated uncertainty in the activation energies is ±5 kcal mol^{-1}.) The fit to the rate of formation predicted by master equation calculations for $C_2H_5 + O_2$ yields a slightly larger apparent activation energy (29.5 kcal mol^{-1}).[20] These rates of formation in the master equation calculations display a strong dependence on the energy of the second transition state between $C_2H_5O_2$ and $C_2H_4 + HO_2$ (−3.0 kcal mol^{-1} as measured from the reactants).[20] Assuming similar R−O_2 bond energies (∼32−37 kcal mol^{-1}),[16] the fact that these three reactions have similar experimentally observed temperature dependences strongly suggests similar energetics for the transition state for HO_2 elimination in these $R + O_2$ reactions. This transition state in $C_2H_5O_2$ is the concerted elimination of HO_2 from a five-membered (CH−OOC) ring structure. However, larger alkyl radicals also have the possibility of forming larger ring structured transition states after O_2 addition that cannot occur in the ethyl + O_2 system. Recent quantum chemistry calculations on $C_2H_5 + O_2$, $C_3H_7 + O_2$, and $C_4H_9 + O_2$ suggest that the HO_2 elimination channel from the five-membered ring transition state is indeed similar for those three reaction systems (with a barrier to HO_2 formation of ∼30 kcal mol^{-1} as measured from the RO_2 well).[39] The present results suggest that a similar concerted elimination dominates HO_2 formation in c-$C_5H_8 + O_2$.

The overall temperature dependence of the prompt yield for cyclopentyl + O_2 (seen in Figure 5) is similar to other $R + O_2$ reactions. The prompt HO_2 yield at lower temperatures appears to decrease with increasing size of the alkyl radical. This trend was previously noted by Kaiser and Wallington[8] for alkene

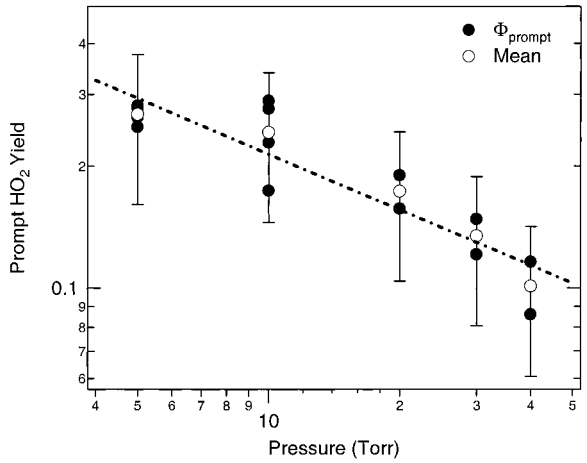

Figure 9. The pressure dependence of the prompt yield of HO_2 from the reaction of c-$C_5H_9 + O_2$ at 638 K and at a constant O_2 density of 6.6×10^{16} molecule cm^{-3}. The mean values are shown as the open circles ○ and the individual determinations as the filled circles ●. The dash−dotted line is the best fit to a P^{-n} dependence, shown for reference.

formation from $C_3H_7 + O_2$ compared to $C_2H_5 + O_2$. They postulated that the smaller alkene yield for $C_3H_7 + O_2$ is due to more efficient stabilization of the propylperoxy radical relative to ethylperoxy due to the additional vibrational degrees of freedom in the propylperoxy radical. Since the cyclopentylperoxy radical is still larger than propylperoxy, it would be expected to give still lower prompt HO_2 yields at low temperature, although the present experimental precision is insufficient to distinguish the difference.

The prompt HO_2 yield produced by the coupled kinetic mechanism is anticipated to be pressure dependent. The decomposition pathway of the adduct to HO_2 and cyclopentene competes with the adduct stabilization pathway. The adduct is stabilized by collisional relaxation with the background gas. An increase in the pressure should increase in the stabilization rate and thus a decrease in the observed prompt yield. Kaiser et al.[8,11−13] have previously established such a pressure dependence for both $C_3H_7 + O_2$ and $C_2H_5 + O_2$. The HO_2 prompt yield from c-$C_5H_9 + O_2$ also shows an inverse pressure dependence as seen in Figure 9.

The initial product yields in the experiments of Handford-Styring and Walker show 9.4% total for acrolein and 1,2-epoxycyclopentane and 87.8% total for cyclopentene and cyclopenta-1,3-diene (from column 1 and 5 of Table 4 in ref 2, with 70 Torr O_2 at 753 K). The cyclopenta-1,3-diene observed is likely formed by further oxidation of cyclopentene, and the total of the two is a measure of the branching ratio of reaction 1b. The total amount of acrolein and 1,2-epoxycyclopentane is an estimate of the branching ratio of the OH producing pathway(s) (represented by reaction 1c). The review of Walker and Morley gives the total initial yield of conjugate alkene to be 90% at 753 K with an initial yield of 87% cyclopentene and 4% cyclopentadiene.[40] These totals imply that ∼10% OH is formed in reaction 1 at 753 K.

In the present study at 723 K the HO_2 yield is still ∼100%, remaining relatively constant after reaching 100% at 683 K. The HO_2 yields corrected only for self-reaction are also near 100% at these temperatures, so the inference of near quantitative conversion to HO_2 does not depend on the assumed c-$C_5H_9O_2 + HO_2$ reaction rate coefficient. This result suggests that no significant additional product channel is opening up at these temperatures. However, the HO_2 yields are consistent with a small amount of OH formation, in the range of what is expected from the experiments of Handford-Styring and Walker (i.e. ≤10%). The OH formed can react with the cyclopentane ($k = 1.84 \times 10^{-11}$ cm^3 molecule^{-1} s^{-1} at 753 K)[2] or with radical species (i.e., OH, HO_2, c-$C_5H_9O_2$, with rate constants ranging from 6×10^{-11} to 10^{-13} cm^3 molecule^{-1} s^{-1}).[14,36] The reaction with cyclopentane forms another cyclopentyl, which then reacts with O_2 to form OH and HO_2. This cycling should continue until all OH is depleted by forming the end product HO_2 or removed from the system by radical−radical reactions. With the initial radical density and cyclopentane concentrations used in this study, simulations show that a 10% contribution of the OH-producing channel could still produce a nearly 100% yield of HO_2. It is interesting to note that Simon et al.[1] do not report any observation of 1,2-epoxycyclopentane formation at the higher temperature of 873 K and explain acrolein formation by secondary reactions without any direct formation from the cyclopentylperoxy. Further studies focused on sensitive real time measurements of OH formation from this reaction are underway and may clarify the role of the adduct in acrolein and 1,2-epoxycyclopentane formation.

Conclusion

The reaction of cyclopentyl radicals with O_2 has been investigated as a function of temperature between 296 and 723 K by using laser photolysis/CW frequency modulation spectroscopy. The overall yield of HO_2 from the cyclopentyl radical + O_2 has been observed as a function of temperature. The HO_2 occurs on two different time scales; a prompt HO_2 signal is observed immediately following the UV flash, and a second slower delayed rise is also observed at higher temperatures. The results from the c-$C_5H_9 + O_2$ reaction are similar to the previous results[3,4] obtained from the $C_2H_5 + O_2$ and $C_3H_7 + O_2$ reactions. Previous work demonstrated that product formation from $C_2H_5 + O_2$ had excellent agreement with the predictions from a coupled kinetics model, where the formation of an ethylperoxy radical is the antecedent to the ethylene + HO_2 formation.[3] The present paper shows a strong similarity of the HO_2 product formation from the reactions of $C_2H_5 + O_2$ and c-$C_5H_9 + O_2$. This similarity suggests that c-$C_5H_9 + O_2$ undergoes a very similar coupled kinetics scheme, where cyclopentylperoxy radical is the antecedent to cyclopentene + HO_2 formation. The apparent activation energies of the three reactions are also very similar, and suggest that the relative energies of the transition states for the concerted HO_2 elimination in the three reactions are similar as well.

Acknowledgment. These experiments described here were made possible by the able technical support of Leonard E. Jusinski. We thank Dr. James A. Miller and Dr. Stephen J. Klippenstein for communicating results prior to publication. This work is supported by the Division of Chemical Sciences, Geosciences, and Biosciences, the Office of Basic Energy Sciences, the U.S. Department of Energy.

References and Notes

(1) Simon, V.; Simon, Y.; Scacchi, G.; Baronnet, F. *Can. J. Chem.* **1997**, *75*, 575.

(2) Handford-Styring, S. M.; Walker, R. W. *J. Chem. Soc., Faraday Trans.* **1995**, *91* (10), 1431.

(3) Clifford, E. P.; Farrell, J. T.; DeSain, J. D.; Taatjes, C. A. *J. Phys. Chem. A* **2000**, *104*, 11549.

(4) DeSain, J. D.; Clifford, E. P.; Taatjes, C. A. *J. Phys. Chem. A* **2001**, *105*, 3205.

(5) Slagle, I. R.; Ratajczak, E.; Heaven, M. C.; Gutman, D.; Wagner, A. F. *J. Am. Chem. Soc.* **1985**, *107*, 1838.

(6) Slagle, I. R.; Park, J.; Gutman, D. *Proc. Combust. Inst.* **1985**, *20*, 733.
(7) Ruiz, R. P.; Bayes, K. D. *J. Phys. Chem.* **1984**, *88*, 2592.
(8) Kaiser, E. W.; Wallington, T. J. *J. Phys. Chem.* **1996**, *100*, 18770.
(9) Kaiser, E. W. *J. Phys. Chem*. **1998**, *102*, 5903.
(10) Gulati, S. K.; Walker, R. W. *J. Chem. Soc., Faraday Trans. 2* **1988**, *84*, 401−407.
(11) Kaiser, E. W. *J. Phys. Chem*. **1995**, *99*, 707.
(12) Kaiser, E. W.; Lorkovic, I. M.; Wallington, T. J. *J. Phys. Chem*. **1990**, *94*, 3352.
(13) Kaiser, E. W.; Wallington, T. J.; Andino, J. M. *Chem. Phys. Lett*. **1990**, *168*, 309.
(14) Atkinson, R.; Baulch, D. L.; Cox, R. A.; Hampson, R. F., Jr.; Kerr, J. A.; Rossi, M. J.; Troe, J. *J. Phys. Chem. Ref. Data* **1997**, *26*, 521.
(15) Kaiser, E. W.; Rimai, L.; Wallington, T. J. *J. Phys. Chem.* **1989**, *93*, 4094.
(16) Knyazev, V. D.; Slagle, I. R. *J. Phys. Chem. A* **1998**, *102*, 1770.
(17) Wagner, A. F.; Slagle, I. R.; Sarzynski, D.; Gutman, D. *J. Phys. Chem*. **1990**, *94*, 1853.
(18) Ignatyev, I. S.; Xie, Y.; Allen, W. D.; Schaefer, H. F., III. *J. Chem. Phys.* **1997**, *107*, 141.
(19) Slagle, I. R.; Feng, Q.; Gutman, D. *J. Phys. Chem*. **1984**, *88*, 3648.
(20) Miller, J. A.; Klippenstein, S. J.; Robertson, S. H. *Proc. Combust. Inst.* **2000**, *28*, 1479; Miller, J. A.; Klippenstein, S. J. The Reaction Between Ethyl and Molecular Oxygen II: Further Analysis; *Int. J. Chem. Kinet.*, in press.
(21) McAdam, K. G.; Walker, R. A. *J. Chem. Soc., Faraday Trans. 2* **1987**, *83*, 1509.
(22) Slagle, I. R.; Ratajczak, E.; Gutman, D. *J. Am. Chem. Soc*. **1985**, *107*, 1838.
(23) Rienstra-Kiracofe, J. C.; Allen, W. D.; Schaefer, H. F., III. *J. Phys. Chem. A* **2000**, *104*, 928.
(24) Pilgrim, J. S.; Taatjes, C. A. *J. Phys. Chem. A* **1997**, *101*, 5776.
(25) Pilgrim, J. S.; Taatjes, C. A. *J. Phys. Chem. A* **1997**, *101*, 4172.
(26) Pilgrim, J. S.; McIlroy, A.; Taatjes, C. A. *J. Phys. Chem. A* **1997**, *101*, 1873.
(27) Pilgrim, J. S.; Taatjes, C. A. *J. Phys. Chem. A* **1997**, *101*, 8741.
(28) Farrell, J. T.; Taatjes, C. A. *J. Phys. Chem. A* **1998**, *102*, 4846.
(29) Herriott, D.; Kogelnik, H.; Kompfner, R. *Appl. Opt*. **1964**, *3*, 523.
(30) Pilgrim, J. S.; Jennings, R. T.; Taatjes, C. A. *Rev. Sci. Instrum.* **1997**, *68*, 1875.
(31) DeMore, W. B.; Sander, S. P.; Golden, D. M.; Hampson, R. F.; Kurylo, M. J.; Howard, C. J.; Ravishankara, A. R.; Kolb, C. E.; Molina, M. J. *Chemical kinetics and photochemical data for use in stratospheric modeling*; **1997**, *12*, JPL Publication 97-4.
(32) Yamasaki, K.; Watanabe, A.; Kakuda, T.; Ichikawa, N.; Tokue, I. *J. Phys. Chem. A* **1999**, *103*, 451.
(33) Yamasaki, K.; Watanabe, A. *Bull. Chem. Soc. Jpn*. **1997**, *70*, 89.
(34) Yamasaki, K.; Watanabe, A.; Kakuda, T.; Tokue, I. *Int. J. Chem. Kinet.* **1998**, *30*, 47.
(35) Rowley, D. M.; Lesclaux, R.; Lightfoot, P. D.; Nozière, B.; Wallington, T. J.; Hurley, M. D. *J. Phys. Chem.* **1992**, *96*, 4889.
(36) Crawford, M. A.; Szente, J. J.; Maricq, M. M.; Francisco, J. J. *J. Phys. Chem. A* **1997**, *101*, 5337.
(37) Rowley, D. M.; Lightfoot, P. D.; Lesclaux, R.; Wallington, T. J. *J. Chem. Soc., Faraday Trans.* **1992**, *88*, 1369.
(38) Lodhi, Z. H.; Walker, R. W. *J. Chem. Soc., Faraday Trans*. **1991** *87*, 681.
(39) DeSain, J. D.; Taatjes, C. A.; Miller, J. A.; Klippenstein, S. J.; Hahn, D. K. "Infrared Frequency-Modulation Probing of Product Formation in Alkyl + O_2 Reactions: IV. Reactions of Propyl and Butyl Radicals with O_2," to appear in *Faraday Discussions*.
(40) Walker, R. W.; Morley, C. In *Low-Temperature Combustion and Autoignition* (Comprehensive Chemical Kinetics Vol. 35); Pilling, M. J., Ed.; Elsevier: Amsterdam, 1997; p 76.